



EUROfusion

WPJET1-PR(18) 21566

A V Chankin et al.

**EDGE2D-EIRENE simulations of the
influence of isotope effects and
anomalous transport coefficients on
near SOL radial electric field**

Preprint of Paper to be submitted for publication in
Plasma Physics and Controlled Fusion



This work has been carried out within the framework of the EUROfusion Consortium and has received funding from the Euratom research and training programme 2014-2018 under grant agreement No 633053. The views and opinions expressed herein do not necessarily reflect those of the European Commission.

This document is intended for publication in the open literature. It is made available on the clear understanding that it may not be further circulated and extracts or references may not be published prior to publication of the original when applicable, or without the consent of the Publications Officer, EUROfusion Programme Management Unit, Culham Science Centre, Abingdon, Oxon, OX14 3DB, UK or e-mail Publications.Officer@euro-fusion.org

Enquiries about Copyright and reproduction should be addressed to the Publications Officer, EUROfusion Programme Management Unit, Culham Science Centre, Abingdon, Oxon, OX14 3DB, UK or e-mail Publications.Officer@euro-fusion.org

The contents of this preprint and all other EUROfusion Preprints, Reports and Conference Papers are available to view online free at <http://www.euro-fusionscipub.org>. This site has full search facilities and e-mail alert options. In the JET specific papers the diagrams contained within the PDFs on this site are hyperlinked

EDGE2D-EIRENE simulations of the influence of isotope effects and anomalous transport coefficients on near SOL radial electric field

A V Chankin¹, G Corrigan², C F Maggi², and JET Contributors*

EUROfusion Consortium, JET, Culham Science Centre, Abingdon, OX14 3DB, UK

¹*Max-Planck-Institut für Plasmaphysik, Garching bei München, Boltzmannstr. 2, 85748, Germany*

²*CCFE, Culham Science Centre, Abingdon, OX13 3DB, UK*

Abstract

EDGE2D-EIRENE (the ‘code’) simulations show that radial electric field, E_r , in the near scrape-off layer (SOL) of tokamaks can have large variations leading to a strong local $E \times B$ shear greatly exceeding that in the core region. This was pointed out in simulations of JET plasmas with varying divertor geometry, where the magnetic configuration with larger predicted near SOL E_r was found to have lower H-mode power threshold, suggesting that turbulence suppression in the SOL by local $E \times B$ shear can be a player in the L-H transition physics [1,2]. Further code modelling of JET plasmas by changing hydrogen isotopes (H-D-T) showed that the magnitude of the near SOL E_r is lower in H cases in which the H-mode threshold power is higher [3]. From the experiment it is also known that hydrogen plasmas have poorer particle and energy confinement than deuterium plasmas, consistent with the code simulation results showing larger particle diffusion coefficients at the plasma edge, including SOL, in hydrogen plasmas [4]. All these experimental observations and code results support the hypothesis that the near SOL $E \times B$ shear can have an impact on the plasma confinement.

The present work analyses neutral ionization pattern of JET plasmas with different hydrogen isotopes in L-mode cases with fixed input power and gas puffing rate, and its impact on target electron temperature, T_e , and SOL E_r . The possibility of a self-feeding mechanism for the increase in the SOL E_r via the interplay between poloidal $E \times B$ drift and target T_e is discussed. It is also shown that reducing anomalous turbulent transport coefficients, particle diffusion and electron and ion heat conductivities, leads to higher peak target T_e and larger E_r , suggesting a possibility of a positive feedback loop, under an implicitly made assumption that the $E \times B$ shear in the SOL is capable of suppressing turbulence.

* See the author list of Litaudon et al, Nucl. Fusion **57** (2017) 102001

1. Introduction

Scrape-off layer (SOL) and divertor make a direct impact on the core region of the plasma via neutral penetration and ionization. While ionization of neutrals is necessary for achieving the desired plasma density in the core, it was known long ago that high large neutral density can lead to the degradation of plasma energy confinement. As was stated in the work by Wagner et al. in 1985, in reference to experimental results of ASDEX and PDX tokamaks in achieving transition from low to high energy plasma confinement regimes (L-H transition) [5]: *‘The detrimental effect of enhanced recycling and gas puffing has been experimentally observed. Both PDX and ASDEX have observed that gas fuelling from the divertor dome instead of the main plasma chamber facilitates the H-transition. Excessive gas puffing can quench the H-mode of PDX yielding low confinement’*. Other (than gas puffing) methods of plasma fuelling, avoiding excessive neutral density at the plasma edge, such as neutral beam injection and deep pellet fuelling, are found to result in desired core density levels without causing confinement degradation. As was recently pointed out by Valovic et al. [6]: *‘A reasonable working hypothesis is that the optimum way to fuel the plasma across the L-H threshold is to increase the plasma density inside the separatrix while minimizing the number of particles deposited in the scrape-off layer’*.

Recent advance in measurement techniques of plasma edge parameters showed that even when neutrals’ ionization doesn’t significantly alter plasma parameter profiles in the core, changing divertor geometry can still make a strong impact on the H-mode power threshold, P_{LH} , (factor two variation in the case of JET plasmas in the ITER-like Wall (ILW) environment, with W diveror and Be main chamber [1,7,8]). The divertor geometry effect on confinement was also seen as the effect of the X-point height (vertical distance between the X-point and the material surface) in JET [9,10], MAST [11], DIII-D [12], Alcator C-mod, where it was referred to as the effect of the outer divertor leg length [13], and COMPASS [14]. All these experiments suggest that there may be other, more subtle mechanisms for the influence of the SOL and divertor on the core plasma, rather than the direct effect of the edge density rise due to neutral ionization. Here it is worth noting that, while the main trends in the parameter dependence of the H-mode power threshold scaling are usually related to core plasma (input power, average density) and engineering parameters (machine size, magnetic field), it is well known that the L-H transition physics is an edge physics process. In the multi-machine Martin’s scaling for the H-mode power threshold [15] there is a large, factor four scatter in experimental data points, apparently due to unaccounted factors/parameters. As pointed out above, only the variation of divertor geometry in JET along causes the factor two variation in P_{LH} .

In search of unaccounted parameters which may explain a large scatter of experimental points for the H-mode power threshold, EDGE2D-EIRENE code [16-18] was used to simulate two JET discharges with different divertor configurations but very similar plasma parameter profiles in the core. It has to be noted that, while EDGE2D-EIRENE is often referred to as a ‘2D fluid edge code’, in reality it is a code package which contains coupled fluid EDGE2D code for plasma behaviour coupled to the Monte Carlo code EIRENE for neutrals.

In one of the simulated discharges the outer strike point was on the horizontal divertor target (HT configuration), while in the other – on the vertical divertor target (VT configuration). Inner strike points were both on vertical targets. Experimentally, in the HT configuration the H-mode power threshold was found to occur at about twice less input power than in the VT configuration. In EDGE2D-EIRENE simulations, the largest difference between the two cases was seen in the E_r profiles at the outer midplane (OMP), originating due to very different target

T_e profiles, see Fig. 4 in ref. [2]. In this figure one can see a very large E_r spike in the near SOL in the HT configuration, and it was hypothesized that the strongly localized $E \times B$ shear in the SOL could suppress turbulence resulting in lower H-mode threshold power.

A substantial difference between near SOL E_r spikes was found in EDGE2D-EIRENE cases with different hydrogen isotopes, with largest spikes for heavier isotopes (the highest – in tritium). This correlates with experimental observations of the lower H-mode power threshold in plasmas with larger average isotope mass [19]. Isotope experiments and modelling will be discussed in more detail in the next section.

In this paper section 2 contains a brief overview of isotope effects on plasma confinement, relevant to the present study. Setup of EDGE2D-EIRENE modelling cases is discussed in Sec. 3. Results of EDGE2D-EIRENE cases are discussed in section 4, including upstream E_r and target parameter profiles (Sec. 4.1), neutral ionization pattern (Sec. 4.2), drift effects (Sec. 4.3), and the influence of varying anomalous transport coefficients on near SOL E_r (Sec. 4.4). Conclusions from the work are drawn in section 5.

2. Isotope effects on plasma confinement

As was pointed out earlier in this paper, the H-mode power threshold is found to be lower in plasmas with heavier hydrogen isotopes. The plasma confinement is typically also worse in H compared to D plasmas (most of the experiments were done in hydrogen and deuterium plasmas). Since modelling results presented in this paper centre on effects of different hydrogen isotopes it is worth giving a brief overview of experimental findings, limited mostly to ASDEX Upgrade and JET L-mode plasmas, and simulations (covering also H-modes, as these results are scarce) with 2D edge codes SOLPS and EDGE2D. Both codes use EIRENE for the description of neutrals behaviour.

One of the first attempts to simulate ASDEX Upgrade experiments, focussing on the difference between plasma edge parameters in large number of H and D plasmas, was made with a variant of SOLPS, B2.5-I, adapted for automatic changes in transport coefficients to match experimental density and temperature profiles at the plasma edge, including SOL [20]. It was found in this study that in H-mode discharges heat conductivities were lower in D plasmas. A thorough analysis of two ASDEX Upgrade H-mode discharges in H and D was carried out in [21] using SOLPS simulations. Perpendicular anomalous diffusion coefficient, D_{\perp} , and electron heat conductivity, χ_e , were established to be lower in the D plasma in both outer core and SOL regions, while ion heat conductivities, χ_i , were the same in H and D plasmas. Minima in transport coefficients were reached at a distance ~ 1 cm inside of the separatrix (at the OMP position). Recently, EDGE2D-EIRENE interpretative simulations were used to compare JET-ILW NBI heated L-modes in H and D in the near separatrix region [4]. Again, larger D_{\perp} was established in the H discharge, less information was available on heat conductivities χ_{ei} due to poorer quality of experimental temperature profiles.

In recent ASDEX Upgrade L-mode experiments with ECRH heating and $T_e > T_i$ it was established that the isotope dependence of energy confinement is a consequence of the mass dependence in the collisional equipartition energy exchange between electrons and ions, as confinement in hydrogen – compared to deuterium – plasmas is accompanied by a larger ion heat flux due to the enhanced electron to ion heat transfer, while the electron transport channel is unaffected by the difference in ion mass [22]. This explanation however is not applicable to

JET-ILW NBI heated L-modes, where ion and electron temperatures are close to each other and the equipartition energy exchange cannot be computed.

Recent EDGE2D-EIRENE simulations of JET ELMy H-mode discharges in H and D with similar stored energies and line-average densities also showed stronger transport barriers for particle and energy fluxes, with transport coefficients being lower in the D discharge. In both cases the minima in transport coefficients were achieved just inside of the separatrix. These discharges however were performed in somewhat different magnetic equilibria.

Summarising, we conclude that available 2D edge code simulations support experimental finding for poorer energy and particle confinement in H compared to D plasmas which is most likely caused by the differences in confinement of the edge plasma. They also show that anomalous transport coefficients are larger in H plasmas not only in the core, but also in the near separatrix and SOL regions. Regarding a possible impact of the near SOL E_r on the plasma confinement described in Sec. 1, there is however no (mostly indirect) evidence that such a link really exists, unless the plasma is close to the L-H transition boundary, where the $E \times B$ shear in the near SOL could potentially accelerate the transition. At the same time, in plasmas with high input power, in particular in H-modes, matching stored energies in H and D requires substantially higher input power in H, leading to larger power flux through the separatrix, higher strike point T_e in the divertor and larger near SOL E_r , indicating the absence of the correlation between the near SOL E_r and confinement. The isotope dependence of the plasma confinement should therefore be attributed to the pedestal physics.

3. Setup of EDGE2D-EIRENE cases

Setup of EDGE2D-EIRENE cases was similar to that described in ref. [3], including the grid which was built based on the magnetic equilibrium of JET pulse #81883 with the outer strike point on the horizontal target (the grid is shown in Figs. 1 and 2 of [3]). All cases were run with drifts and parallel currents. A self-consistent neoclassical model for E_r was implemented in the core which impeded surface averaged radial currents. Only pure hydrogen isotope cases (in H, D and T) were run, without impurities. The material surfaces were assumed as in the ITER-like Wall (ILW). The EIRENE version with Kotov-2008 model was used to describe neutral behaviour. Spatially constant anomalous transport coefficients were specified: diffusion coefficient $D_{\perp}=1 \text{ m}^2\text{s}^{-1}$ and electron and ion heat conductivities $\chi_{e,i}=2 \text{ m}^2\text{s}^{-1}$ across the whole grid, unless otherwise stated. The input power into the grid was set at 3.0 MW, split equally between ion and electron channels.

In difference to cases described in ref. [3], however, where plasma density was controlled by a combination of gas puff and wall recycling ('puff + recycling' option in EDGE2D-EIRENE), aiming at maintaining a specified electron density at the outer midplane (OMP) position of the separatrix, $n_{e,sep}$, the fixed gas puff from the top of the machine, at $4.2 \times 10^{21} \text{ s}^{-1}$, was used in this study. This level of the gas puff corresponded to the case in deuterium described in [3]. The change from fixing $n_{e,sep}$ to constant gas puff for all isotopes was done in order to get an insight into physics governing particle confinement in plasmas with different hydrogen isotopes. Since in the experiment H discharges are found to require larger gas puff to reach the same line-average density as in D discharges, indicating poorer particle confinement in H, the question arises whether for the same gas puff in H as in D the near SOL E_r is smaller in H. In such a case the hypothesis that the $E \times B$ shear in the SOL can suppress turbulence leading to better particle confinement would be strengthened. In earlier isotope scans, described in [3], gas puff levels had to be increased going from T to H in order to maintain the same $n_{e,sep}$. This

caused somewhat higher radiation power losses for lighter isotope plasmas, contributing to lower peak target T_e and near SOL E_r . The present setup is therefore more challenging for obtaining higher near SOL E_r in heavier isotope plasmas.

Finally, the newest version of EDGE2D-EIRENE was used in this study, which however caused only very minor changes in output profiles of plasma parameters compared to the earlier version used in cases described in ref. [3].

4. EDGE2D-EIRENE cases and analysis

There were two main motivations for running EDGE2D-EIRENE cases in this study. The first was to establish whether in heavier hydrogen isotopes, for the same level of the gas puff, the spike of the near SOL E_r is larger, and if so, to understand the physics of this phenomenon. The second motivation was to test the effect of varying transport coefficients on the near SOL E_r . If the near SOL E_r is indeed larger in heavier isotopes, one would then expect stronger turbulence suppression in the SOL by the $E \times B$ shear and an improvement in particle and energy confinement. This would then justify using lower transport coefficients in cases with heavier isotope plasmas. If, in turn, lower transport coefficients result in larger near SOL E_r , a positive feedback loop can be created leading to more substantial difference between plasmas in H, D and T.

4.1 OMP E_r and target profiles in isotope scan cases

In this section the output from EDGE2D-EIRENE isotope scan cases with exactly the same setup are described. In particular, H, D and T cases were run with the same transport coefficients and the same gas puff. Fig. 1 shows OMP profiles of n_e , T_e and T_i vs. distance from the separatrix. The largest difference between H, D and T cases is in density profiles, especially near the separatrix position and in the SOL. Separatrix density $n_{e,sep}$ is higher in the T case compared to the H case by factor 1.187, and the difference in density gradients at the separatrix position is factor 1.39 larger in favour of the H case. For the same transport coefficients this implies that particle flux across the separatrix is by factor 1.39 larger in H than in D. This can be explained by deeper penetration of lightest, H neutrals, into the plasma and its stronger ionization source in the core. Since most of the ionization takes place within the simulation domain (EDGE2D grid), in the steady state conditions, achieved in each of the cases, ionization source in the core must be compensated by the plasma particle flux across the separatrix from the core into the SOL, which is largest in the H case.

Outer midplane (OMP) E_r profiles for all three cases are shown in Fig. 2. There is a very little difference between these profiles in the core, and E_r is almost constant for all cases there. The only significant feature of the E_r profiles, capable of creating large $E \times B$ shear, is in the SOL, and in particular, positive E_r spikes in the near SOL. The spike is largest in the T case and lowest in the H case.

Profiles of E_r in the core region are rather flat. This is due to flatness of ion pressure and T_i profiles which determine E_r in the neoclassical theory, provided there is no large toroidal momentum (which was assumed to be zero at the inner core boundary for all cases presented in this paper). Plasma transport equations in EDGE2D assume strong collisionality Pfirsch-Schlüter regime for both SOL and core plasma conditions. In the core, however, this assumption is at least marginal, and is often violated, with the collisionality regime becoming Plateau. The coefficient K which accounts for the contribution of the T_i gradient to the neoclassical E_r , given by $k \nabla T_i / en$, depends on the collisionality regime, being the largest in the

Pfirsch-Schlüter regime [23]. If the EDGE2D model was more realistic, by e.g. also covering the Plateau region, it would then yield less flat profiles, with lower E_r just inside of the separatrix, qualitatively consistent with experimental observations of the E_r ‘well’ just inside of the separatrix seen in experiments (see e.g. ASDEX Upgrade results in [24]).

Target profiles of n_e , T_e and T_i for all three cases are shown in Figs. 3a, b and c, respectively. Target densities are lowest in the H case, which can be explained by higher velocity of H neutrals and lower ionization source in the SOL (see analysis of ionization sources in the next sub-section). This also makes its impact on $n_{e,sep}$, which is lowest in the H case, as discussed above. Peak T_e at the outer target (OT) is highest in the D case. This doesn’t contradict to the fact that the highest peak E_r is seen in the T case, since it is the radial T_e gradient, rather than the T_e itself, which gives the largest contribution to the upstream E_r , as follows from the explanation of the origin of E_r based on the effect of the Debye sheath potential drop $\sim 3T_e/e$ [25], under conditions of constant target potential (the target in these EDGE2D-EIRENE cases was assumed to be made of tungsten, hence, the target potential was radially constant). Since electron temperatures at the inner target (IT) are very low near the strike point, they make a negligible contribution to the formation of the upstream E_r . Target T_i profiles, similarly to target T_e profiles, are substantially larger for D and T cases than for the H case. Note that the target T_e , as well as T_i , are lowest in the H case only near the strike point, whereas further out in the SOL they are, on the contrary, the highest among the three cases.

4.2. Neutral ionization pattern in isotope scan cases

The total ionization source for each poloidal ring, summed up over all cells, from outer to inner target for SOL rings, and along the whole poloidal transit for core cells, vs. OMP cell centre positions relative to the separatrix position, is plotted in Fig. 4a, and its expansion around the separatrix position is plotted in Fig. 4b. Calculation of these quantities requires multiplication of ionization density (in $m^{-3}s^{-1}$) by the cell volume, cell by cell, and summing up the results over all cells. Neutral ionization occurs mostly in the divertor. Ionization source in the core is largest in the H case, as expected, and consistent with n_e profiles shown in Fig. 1.

The characteristic penetration length of neutrals into the core is difficult to calculate using quantities described just above owing to the 2D nature of the ionization pattern, with maxima of the total ionization reached near the X-point position due to the large flux expansion there. Because of such a significant contribution of the X-point region, ionization density decay lengths extracted from average ionization rates obtained by dividing total ionization sources in poloidal rings by ring volumes didn’t have much physical sense. In the core region, e-folding decay lengths of average ionization rates from the separatrix to the inner core boundary are calculated to be 1, 1.35 and 2.05 cm for H, D and T cases respectively, clearly in breach of the expected inverse square isotope mass dependence based on neutrals’ velocities for a given energy. This is caused entirely by the largest ionization source in the X-point region of the H case, and the lowest – in the T case, as seen in Figs. 4a,b, as discussed below. At the same time, local ionization rates along the OMP position qualitatively obey the expected isotope mass dependence: e-folding decay lengths across the core region are 4.6, 3.1 and 2.4 cm for H, D and T cases respectively.

Figs. 5a,b show poloidal distributions of ionization sources against cell row numbers for the first ring in the SOL (ring S01, according to the EDGE2D nomenclature, Fig. 5a) and for the last ring in the core, closest to the separatrix (ring C01, according to the EDGE2D nomenclature, Fig. 5b). Row numbers give numbers of cells in the poloidal direction. For SOL

rings numbering starts from the OT, while for core rings it starts from the bottom of the grid. In either case the poloidal cell numbering adopted in EDGE2D is counter-clockwise. Profiles shown in Figs. 5a,b give total ionization sources for each cell, including the cell volume. Maxima of ionization sources seen in Fig. 5a, especially large in the H case, correspond to cell positions close to the X-point. The same is true for profiles shown in Fig. 5b. Note that the number of cells is larger for ring S01, since this ring includes cells in the divertor in difference to the ring C01 which covers the core. Poloidal profiles of the same quantity for rings S02 and C02, further away from the separatrix in the SOL and core, respectively, show qualitatively similar but less pronounced patterns.

The reason for large contributions from cells near the X-point can be seen from Fig. 6 which shows the expanded view of the EDGE2D grid in the divertor and the bottom of the core region. Due to large poloidal flux expansion around the X-point, EDGE2D grid cells around this position are larger than other cells. Consequently, the ionization source is largest in these cells. Among the three isotopes, hydrogen atoms, having the highest velocity, have largest probability to reach these cells, while for D and T larger proportion of neutrals gets ionized before reaching these cells. This explains why the H case has stronger ionization in the near SOL rings, adjacent to the separatrix, and weaker ionization in the far SOL, which gives rise to flatter T_e profiles along OT and lower E_r spikes at OMP.

4.3. Drift effects in isotope scan cases

Understanding certain features of target profiles shown in previous sub-sections require consideration of drifts effects, especially the effect of the poloidal $E \times B$ drift caused by radial electric field and directed from the IT to OT for positive E_r , which is correct for the ‘forward’ toroidal field direction with the ion ∇B drift down, towards the X-point, which was the case in all EDGE2D-EIRENE cases discussed in this paper. In the presence of drifts, some commonly used assumptions, such as conservation of total, ion plus electron pressure along field lines in the absence of parallel momentum losses, or the $T_e^{7/2} / L_{\parallel}$ law for parallel heat flux, where T_e is upstream (e.g. OMP) electron temperature and L_{\parallel} - parallel distance between the upstream position and the target [25], don’t apply. This is because poloidal $E \times B$ drift carries both particle and (convective) power fluxes towards the OT (for positive E_r and ‘forward’ toroidal field direction). Target profiles in the hydrogen scan cases were strongly affected by poloidal $E \times B$ drift.

Fig. 7 shows an expanded view, zoomed around the outer strike point position, of the E_r profile at the OMP and n_e and T_e profiles at OT of the isotope scan cases vs. distance from the separatrix position mapped to the OMP. For target profiles, distances were mapped to the OMP position along field lines. There is one missing point on the OMP E_r profile, at the 1st SOL ring S01. E_r points at this location are also absent in Fig. 2, but there it is less noticeable. The reason why these points aren’t plotted is related to the procedure of the calculation of E_r values in the SOL and in the core. In the SOL, electric potential is the primary quantity. It is possible to calculate it since there is a reference point for the potential, which is assumed to be zero at (conducting, as in these cases) divertor targets. E_r is then calculated by subtracting electric potentials from the neighboring rings. In contrast, in the core the primary quantity is E_r , which has values that ensure ambipolarity of drift-related surface averaged radial (normal to flux surfaces) plasma fluxes. Since core and SOL regions are topologically separated from each other, it is impossible to connect electric potentials in them, unless one uses some model for electric currents through the separatrix. Such a model is not used in EDGE2D, instead, it is

assumed that electric potentials in the last (outermost) core ring C01 and the first (innermost) SOL ring S01 are equal to each other, hence E_r across the separatrix is assumed zero. Since the calculation of E_r for the SOL ring S01 requires subtraction between electric potentials in rings C01 and S02, taking into account a rather arbitrary connection between potentials in the core and SOL, such a procedure doesn't give physically sensible E_r values. For this reason E_r values for the ring S01 are not plotted.

The primary quantity which determines relative changes in E_r and electron density n_e for the three isotopes shown in Fig. 7, is electron temperature T_e . It shows a much flatter profile for H than for D and T for the first few rings just outside of the separatrix. Large E_r differences between these cases are mostly the consequence of the differences in target T_e profiles. Since positive E_r values in the SOL result in poloidal plasma fluxes towards the OT (in these cases, for the give toroidal field direction), they cause the plasma compression at OT. This leads to larger n_e at OT. The $E \times B$ compression also causes the T_e rise at OT, which is explained just below. Owing to the coefficient $5/2$ (instead of $3/2$) in the expression for the convective power flux, $5/2\Gamma T$, where Γ is particle flux and T is temperature, which equally applies to parallel and cross-field fluxes, plasma compression at the OT by the poloidal $E \times B$ drift causes increase of both plasma density and temperature. It can be easily shown that the effect of such a compression gives a fairly high rate of the temperature increase, equal to $2/3$'s of that for density: $\frac{dT}{Tdt} = \frac{2}{3} \frac{dn}{dt}$. This, in addition to the tendency for lower target n_e in the H case discussed earlier, further increases target T_e in the first two poloidal rings in D and T cases compared to the H case. There may therefore exist a positive feedback loop between the near SOL E_r and target T_e , where poloidal $E \times B$ drift increases target T_e , which, in turn, increases E_r in the SOL.

The impact of the poloidal $E \times B$ drift on the power flux into the outer divertor is illustrated in Fig. 8. Solid lines show total, ion plus electron, convective plus conductive, power flux through the cell face boundary indicated by thick red line in Fig. 6, at the SOL ring S01. This boundary is two rows of cells above another boundary separating 'divertor SOL' (using EDGE2D nomenclature) from the outer divertor. The power flux through it collects almost all radial power flux crossing the separatrix through the outboard (lower filed) side, at the same time, the power crossing this boundary is not much affected by power sinks in the divertor and large cells surrounding the X-point. Dashed lines in Fig. 8 show only convective ion plus electron power flux through the same boundary. It is clear that convective power fluxes in the near SOL make a significant contribution to the total power fluxes. Convection is also responsible for the modulation of the shape of the total power flux profiles in the SOL. The modulation is clearly caused by the modulation of the shape of the E_r profile shown in Fig. 2.

There is one extra factor supporting drift effects in the near SOL. In SOL rings closest to the separatrix, owing to the large flux expansion near the X-point field lines are longer, hence the parallel conductive power flux $T_e^{7/2} / L_{\parallel}$ is lower. For example, for the 1st ring outside of the separatrix, the distance from the outer to inner target along the field line is 119.2 m, for the 3rd ring – 109.2 m, for the 5th ring – 96.6 m, and for the last, 20th ring – 77.5 m. At the same time, electric potential distribution at the OMP is unaffected by long L_{\parallel} . Hence, the relative contribution of the convective power flux carried by the poloidal $E \times B$ drift is stronger than at other, more outward positions in the SOL. Another contribution towards the increase of a relative contribution of convection to total power fluxes is higher T_i than T_e , which is often the

case in the ‘main’ SOL, upstream of the divertor. In the cases shown here the T_i/T_e ratio at the cell face boundary for which power fluxes are plotted in Fig. 8 is ≈ 1.4 , which increases the contribution of ion convective power fluxes.

4.4. Influence of transport coefficients on near SOL E_r

As was pointed out in Sec. 3, all cases were run with the same anomalous transport coefficients for all isotopes. Since particle and energy confinement, as well as transport coefficients at the plasma edge extracted from fluid 2D edge code simulations, indicate better confinement in plasmas with heavier hydrogen isotopes (see Sec. 2), the question arises whether specifying the same transport coefficients for all isotope runs is realistic. The motivation for using the same transport coefficients was explained at the beginning of Sec. 4. However, once the cause of isotope effects on the near SOL E_r has been established, one can explore a possibility of the near SOL E_r , via its effect on turbulence suppression, reducing transport coefficients. This effect could amplify isotope effects on the confinement.

E_r profiles for the isotope scan cases with variable transport coefficients are shown in Figs. 9a-c. The D case is the original case, for which results were shown in previous figures. For H and T cases transport coefficients were changed according to the $\sqrt{m_D/m_i}$ scaling, where m_i is either H or T mass. The square root dependence is chosen based on the results of EDGE2D-EIRENE simulations for JET L-mode plasmas, which established that in the D discharge D_\perp in the SOL was by factor 1.4 lower in the D than in the H discharge [4]. Fig. 9a shows the same profiles for original (same for all isotopes) transport coefficients, it only differs from Fig. 2 by the vertical scale which is adjusted to be the same as in Figs. 9b,c. Fig. 9b shows results of varying only D_\perp by factor $\sqrt{m_D/m_i}$. Fig. 9c shows results of varying both D_\perp and $\chi_{e,i}$ by this factor. It is clear from Figs. 9a-c that reducing transport coefficients, mostly D_\perp , leads to an increase in the near SOL E_r . For the T cases, the E_r spike, measured as the difference between the maximum E_r value in the SOL and its value at the core ring closest to the separatrix, is larger in Fig. 9c than in Fig. 9a by factor 1.48. For the H cases, the same quantity is smaller by factor 1.42 in Fig. 9c than in Fig. 9a. The near SOL E_r spikes in these cases therefore appear to scale approximately as $\sqrt{m_i/m_D}$, that is, inversely proportional to the variation in transport coefficients.

Another test was made using only D cases. Fig. 10 shows the effect of varying all transport coefficients by factors 2: starting with the original transport coefficients, they were multiplied by factors 2 and $1/2$. A very strong impact of such a variation of transport coefficients on the near SOL E_r spikes can be seen in the figure. Target T_e profiles for the same cases as shown in Fig. 10, are shown in Fig. 11. Convective and total power fluxes near the entrance to the outer divertor for these cases are shown in Fig. 12. In black (marked ‘orig_case’) are the same fluxes as shown in Fig. 8 for the D case, while in red (marked ‘coef_x0.5’) and blue (marked ‘coef_x2’) are D cases with transport coefficients multiplied by factors 0.5 and 2, respectively.

Results of this sub-section show that positive feedback loops amplifying the influence of the near SOL E_r on the $E \times B$ shear turbulence suppression may be considered, both for the formation of the $E \times B$ shear and for its effect on transport coefficients in the SOL.

5. Conclusions

Possible turbulence suppression by the $E \times B$ shear in the near SOL is likely to be an additional mechanism responsible for large scatter in experimental data on the H-mode power threshold (factor two in JET-ILW plasmas, depending on the divertor configuration), rather than be responsible for main trends in this threshold as described by power threshold scalings. Recent findings from AUG seem to have provided convincing evidence that scalings for the H-mode threshold power, in particular the Martin scaling [15], are related to the threshold in the ion power flux through the separatrix [26], which is not directly related to divertor target T_e profiles and E_r in the SOL. At the same time, the above findings don't explain the dependence of the H-mode threshold power (P_{LH}) on extreme edge region, as evidenced by the strong influence of the divertor configuration on P_{LH} . It is therefore quite possible that the extreme edge, in particular SOL and divertor regions, can make a strong impact on P_{LH} and account, at least partly, for a large scatter of experimental P_{LH} (factor four scatter as seen in Ref. [15]).

Analysis of possible physical mechanisms for the influence of hydrogen isotope effects on the plasma particle and energy confinement in the plasma core is beyond the scope of the present paper. It focuses on the extreme edge region, in particular, separatrix and near SOL regions, and a possible influence of the near SOL E_r on the turbulence suppression in the SOL. EDGE2D-EIRENE modelling of hydrogen isotope scan cases shows that different neutral ionization patterns, depending on the isotope, may be responsible for the difference in the near SOL E_r . It is well known that the largest neutral circulation takes place in the divertor, causing large ionization source there. The remaining neutrals, which weren't ionized in the divertor, can penetrate (mostly) into the core and be ionized there. Large plasma volume around the X-point location presents a strong barrier for neutrals on their way to the core. The lightest isotope, hydrogen, has the largest probability to reach the X-point region and get ionized in the 1st poloidal ring, just outside of the separatrix. This ionization increases n_e and reduces T_e in this ring at the target, leading to lowest near SOL E_r out of the three isotope cases.

The effect of the poloidal $E \times B$ drift may amplify the initial difference in the near SOL E_r between EDGE2D-EIRENE cases for different isotopes caused by the difference in the ionization pattern. The extra convective poloidal power flux associated with the poloidal $E \times B$ drift causes higher target $T_{e,i}$, which in turn result in larger near SOL E_r . Such a self-amplifying effect may create larger difference in near SOL E_r for cases with different isotopes compared to those caused only by the ionization patterns.

A potential positive feedback loop with a possible impact on the near SOL E_r was identified in the modelling. In a series of cases in deuterium with different anomalous transport coefficients larger near SOL E_r spikes are found in cases with lower transport coefficients. The larger near SOL E_r in turn can result in turbulence suppression by the poloidal $E \times B$ shear. In relation to the isotope scan cases, variation of transport coefficients by factor $1/\sqrt{m_i}$ led to the increase in the near SOL E_r spikes by approximately factor $\sqrt{m_i}$. Thus, again, a self-amplifying mechanism may be considered by which edge plasmas with heavier hydrogen isotopes may end up having stronger turbulence suppression and lower transport coefficients.

Acknowledgement

This work has been carried out within the framework of the EUROfusion Consortium and has received funding from the Euratom research and training programme 2014-2018 and 2019-2020 under grant agreement No 633053. The views and opinions expressed herein do not

necessarily reflect those of the European Commission. Discussions with Dr. A. Jarvinen are acknowledged.

References

- [1] Delabie E *et al.* 2015 *42nd EPS Conf. on Plasma Physics* (Lisbon, Portugal, 22–26 June 2015) paper O3.113 (<http://ocs.ciemat.es/EPS2015PAP/pdf/O3.113.pdf>)
- [2] Chankin A V *et al.* 2017 *Nucl. Materials and Energy* **12** 273
- [3] Chankin A V *et al.* 2017 *Plasma Phys. Control. Fusion* **59** 045012
- [4] Maggi C F *et al.* 2018 *Plasma Phys. Control. Fusion* **60** 014045
- [5] Wagner F *et al.* 1985 *Nucl. Fusion* **25** 1490
- [6] Valovič *et al.* 2012 *Nucl. Fusion* **52** 114022
- [7] Maggi C *et al.* 2014 *Nucl. Fusion* **54** 023007
- [8] Meyer H *et al.* 2014 *41st EPS Conf. on Plasma Physics*, (Berlin, Germany, 23–27 June 2014) paper P1.013 (<http://ocs.ciemat.es/EPS2014PAP/pdf/P1.013.pdf>)
- [9] Horton L D 2000 *Plasma Phys. Control. Fusion* **42** A37–49
- [10] Andrew Y *et al.* 2004 *Plasma Phys. Control. Fusion* **46** A87-93
- [11] Meyer H *et al.* 2011 *Nucl. Fusion* **51** 113011
- [12] Gohil P *et al.* 2011 *Nucl. Fusion* **51** 103029
- [13] Ma Y, Hughes J W, Hubbard A E, LaBombard B and Terry J 2012 *Plasma Phys. Control. Fusion* **54** 082002
- [14] Dejarnac R *et al.* 2016 *25th IAEA Fusion Energy Conf.* 17-22 Oct., paper No. OV/P-3
- [15] Martin Y *et al.* 2008 *J. Phys.: Conf. Ser.* **123** 012033
- [16] Simonini R *et al.* 1994 *Contrib. Plasma Phys.* **34** 368
- [17] Reiter D 1992 *J. Nucl. Mater.* **196-198** 80
- [18] Wiesen S *et al.* 2006 ITC Project Rep. (http://www.eirene.de/e2deir_report_30jun06.pdf)
- [19] Righi E *et al.* 1999 *Nucl. Fusion* **39** 309
- [20] Kim J-W *et al.* 2001 *J. Nucl. Mater.* **290-293** 644
- [21] Horton L D *et al.* 2005 *Nucl. Fusion* **45** 856
- [22] Schneider P A *et al.* 2017 *Nucl. Fusion* **57** 066003
- [23] Hazeltine R D 1974 *Phys. Fluids* **17** 961.
- [24] Viezzer E *et al.* 2014 *Nucl. Fusion* **54** 012003
- [25] Stangeby P C 2000, *The Boundary of Magnetic Fusion Devices*, IOP Publishing, Bristol
- [26] Ryter F *et al.* 2014 *Nucl. Fusion* **54** 083003

Figures

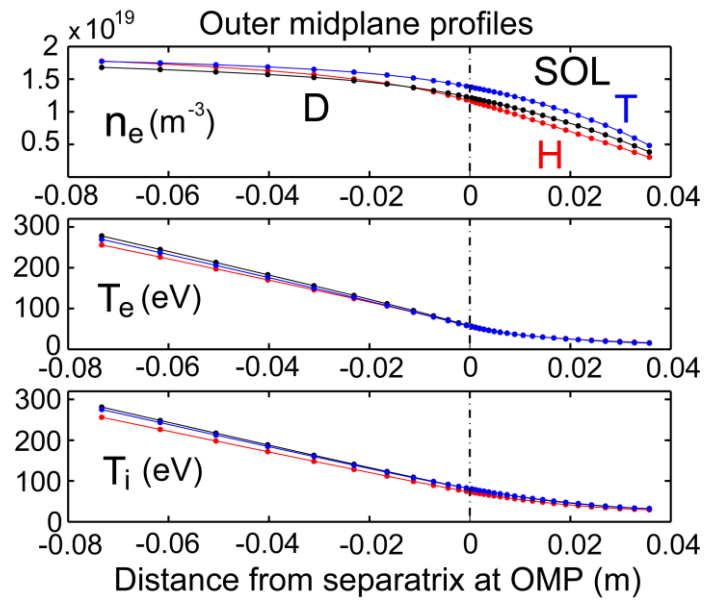


Fig. 1. Outer midplane (OMP) profiles of n_e , T_e and T_i vs. distance from the separatrix for EDGE2D-EIRENE cases in hydrogen (H), deuterium (D) and tritium (T).

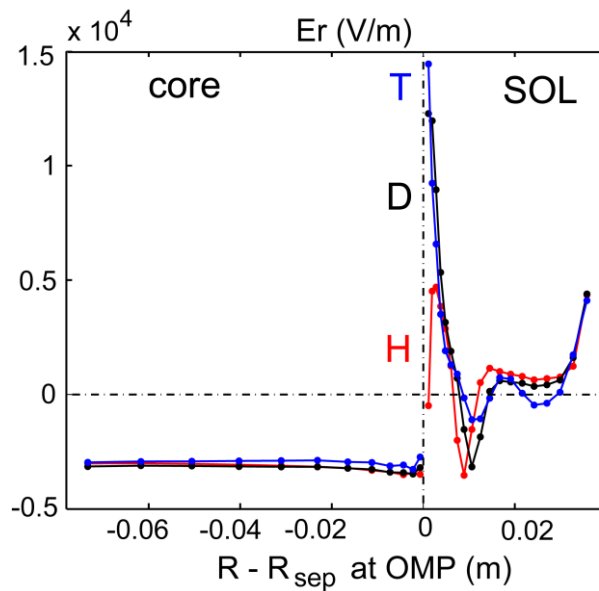
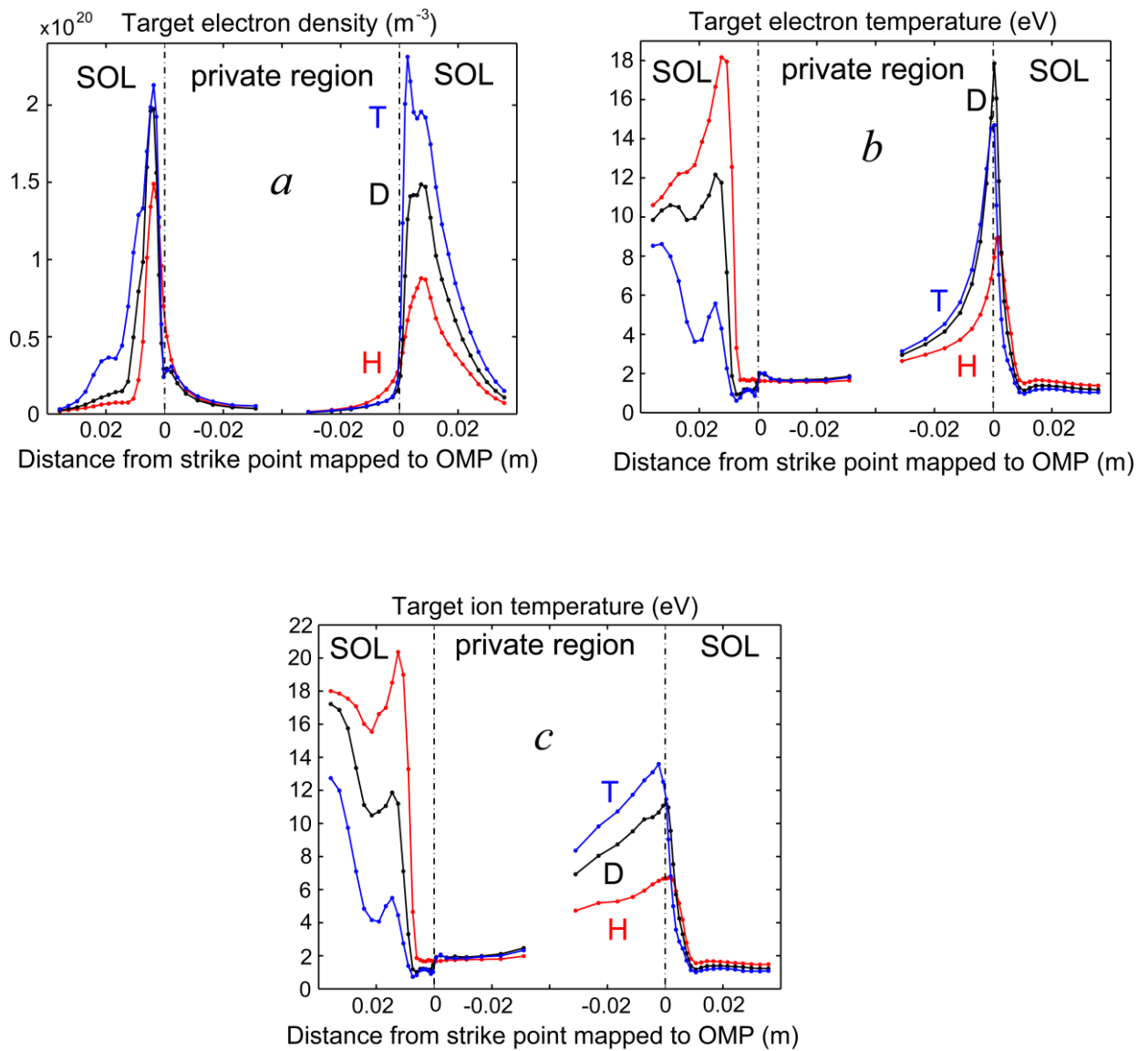
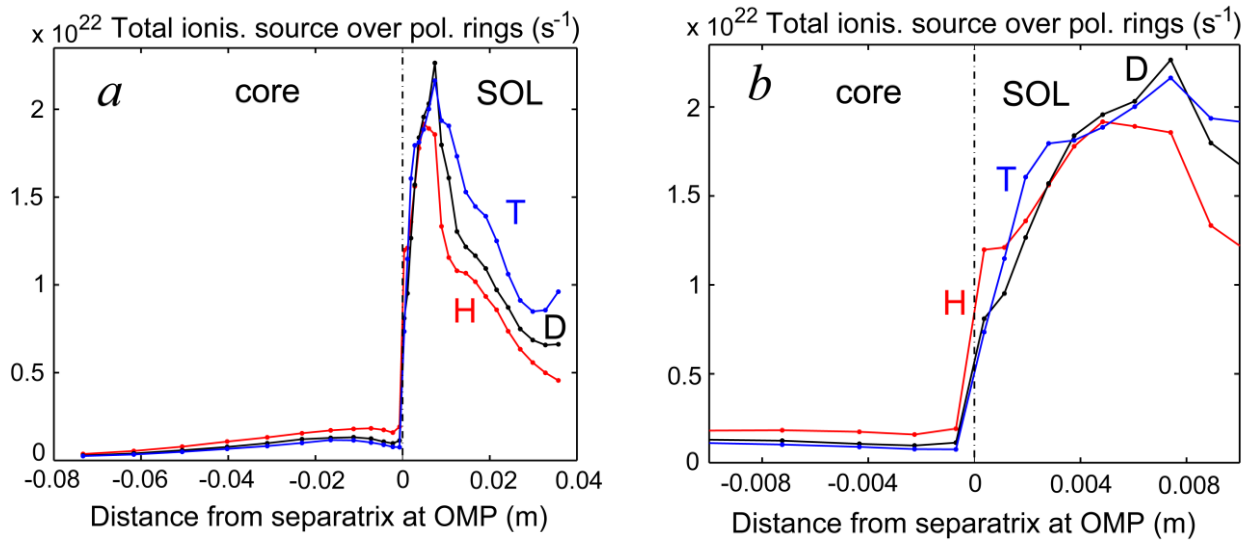


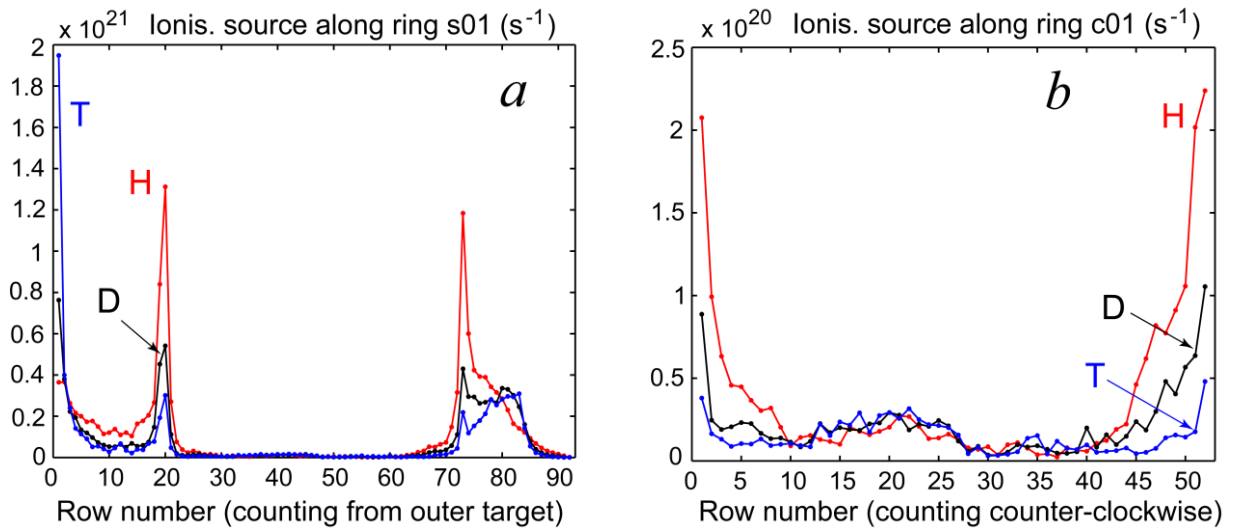
Fig. 2. Outer midplane (OMP) E_r profiles for the three hydrogen isotope cases vs. distance from the separatrix.



Figs. 3a-c. Target profiles of n_e (a), T_e (b) and T_i (c) for the three hydrogen isotope cases vs. distance from the strike point mapped to the OMP position along field lines.



Figs. 4a,b. Total ionization source for each poloidal ring, summed up over all cells, from outer to inner target, for all SOL rings vs. OMP cell centre positions relative to the separatrix position (a), and the same plot expanded around the separatrix position (b).



Figs. 5a,b. Poloidal distributions of ionization sources against cell row numbers for the first ring in the SOL, ring $S01$ (a), and for the last ring in the core, ring $C01$ (b). See text for details.

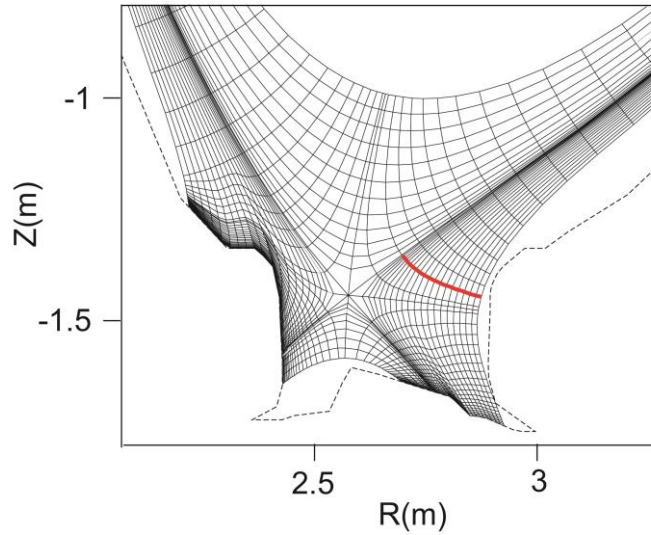


Fig. 6. Expanded view of the EDGE2D grid in the divertor and the bottom of the core region.

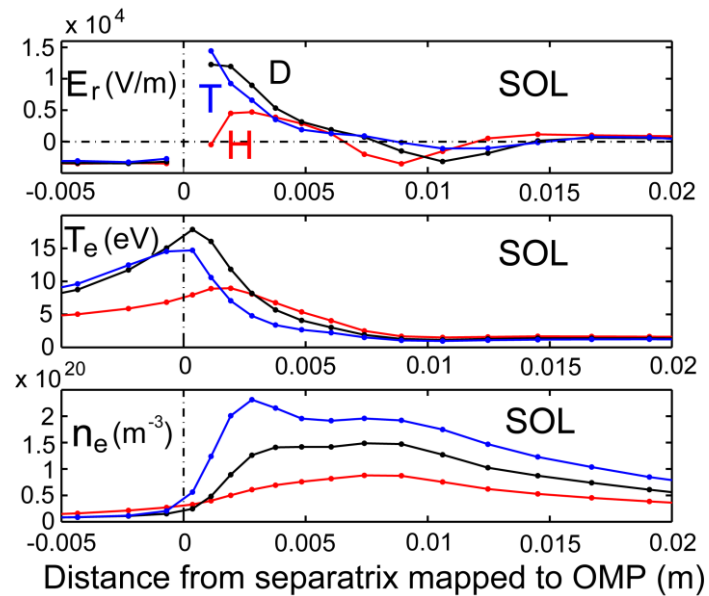


Fig. 7. Expanded view, zoomed around the outer strike point position, of the E_r profile at the OMP and n_e and T_e profiles at outer target (OT) of the isotope scan cases vs. distance from the separatrix position mapped to the OMP position along field lines.

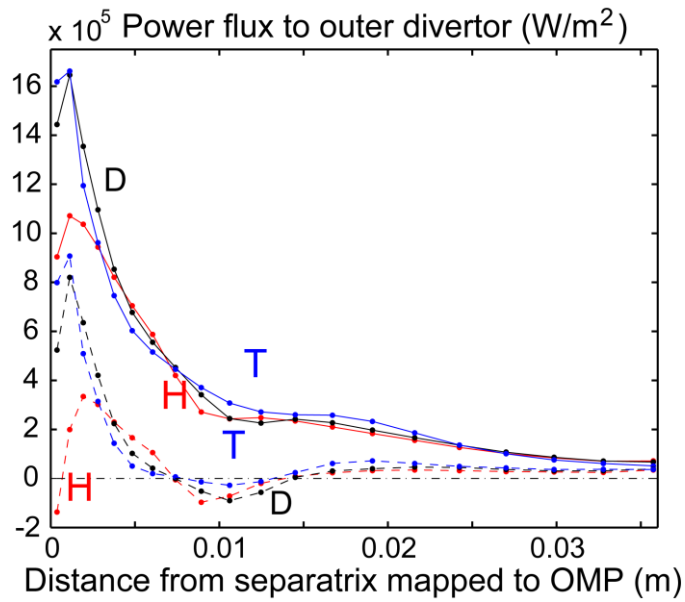
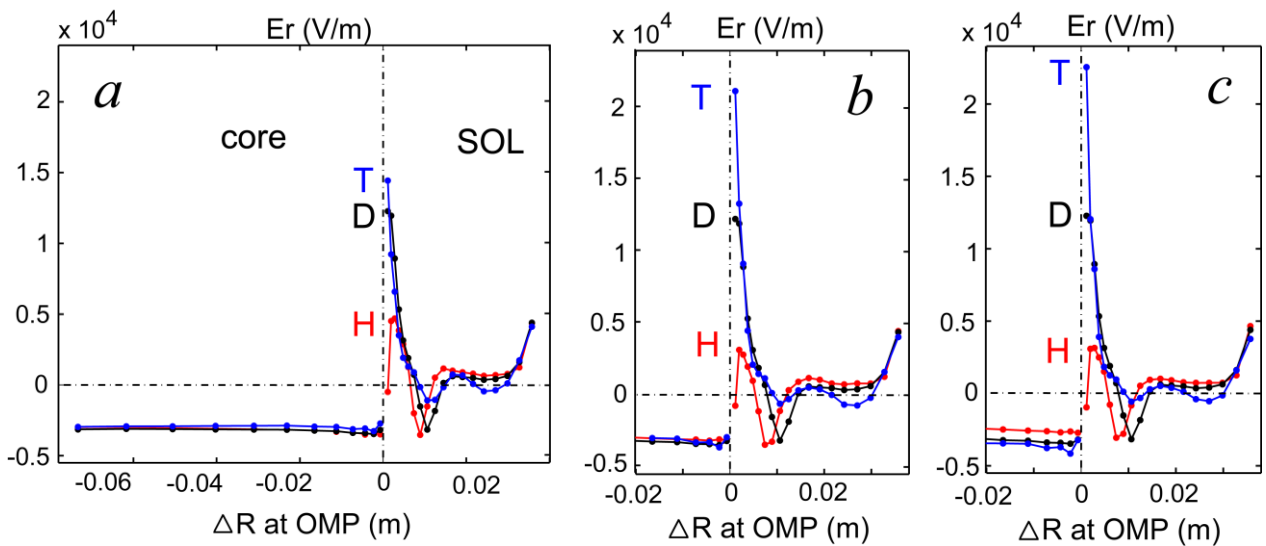


Fig. 8. Total, ion plus electron, convective plus conductive, power flux through the cell face boundary indicated by thick red line in Fig. 6, at the SOL ring S01 (solid lines), and only convective ion plus electron power flux through the same boundary (dashed lines).



Figs. 9a-c. E_r profiles for the isotope scan cases with variable transport coefficients vs. distance from the separatrix at the OMP position. The D case in all figures is the original isotope scan case, for which results were shown in previous figures. For H and T cases transport coefficients were changed. See text for details.

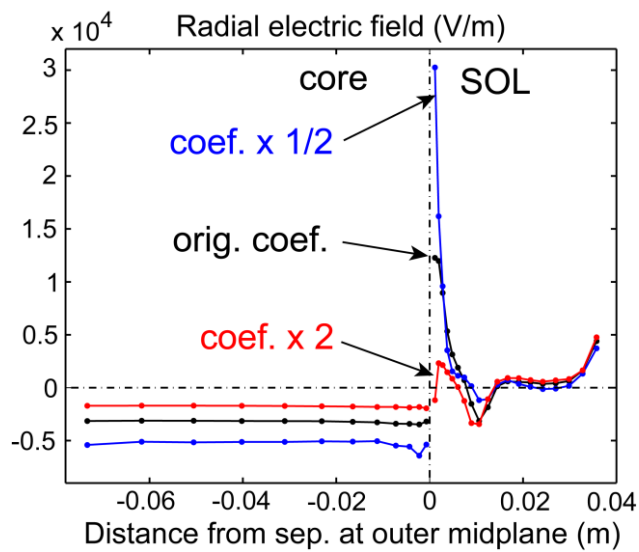


Fig. 10. Effect of varying all transport coefficients by factors 2 on E_r at the OMP vs. distance from the separatrix at the OMP position: starting with the original transport coefficients, they were multiplied by factors 2 and $\frac{1}{2}$.

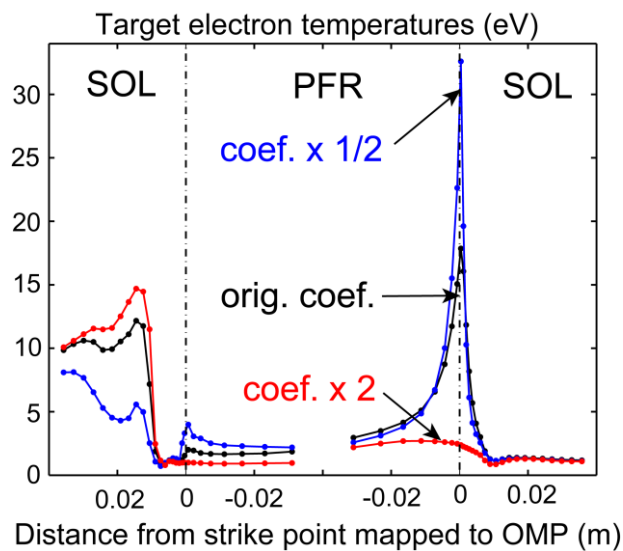


Fig. 11. Target T_e profiles for cases shown in Fig. 10, mapped to the OMP position along field lines.

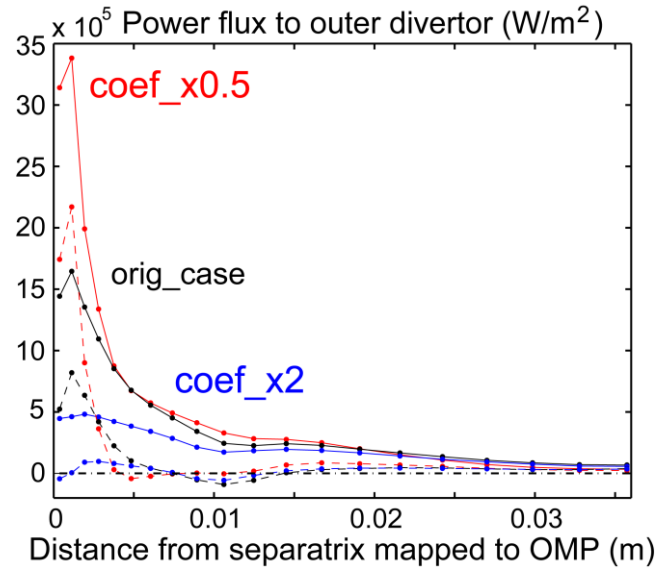


Fig. 12. Total, ion plus electron, convective plus conductive, power fluxes through the cell face boundary indicated by thick red line in Fig. 6, at the SOL ring S01 (solid lines), and only convective ion plus electron power flux through the same boundary (dashed lines). The case in D (in black, marked 'orig_case') is the same as shown in Fig. 8, while cases marked 'coef_x0.5' (in red) and 'coef_x2' (in blue) are D cases run for all transport coefficients multiplied by factors 0.5 and 2, respectively.